INFLUENZA

Circulating T_{FH} cells, serological memory, and tissue compartmentalization shape human influenza-specific B cell immunity

Marios Koutsakos,[1] Adam K. Wheatley,[1] Liyen Loh,[1] E. Bridie Clemens,[1] Sneha Sant,[1] Simone Nüssing,[1] Annette Fox,[1] Amy W. Chung,[1] Karen L. Laurie,[2] Aeron C. Hurt,[2] Steve Rockman,[1,3] Martha Lappas,[4] Thomas Loudovaris,[5] Stuart I. Mannering,[5] Glen P. Westall,[6] Michael Elliot,[7,8] Stuart G. Tangye,[9,10] Linda M. Wakim,[1] Stephen J. Kent,[1,11,12] Thi H. O. Nguyen,[1*†] Katherine Kedzierska[1*†]

Immunization with the inactivated influenza vaccine (IIV) remains the most effective strategy to combat seasonal influenza infections. IIV activates B cells and T follicular helper (T_{FH}) cells and thus engenders antibody-secreting cells and serum antibody titers. However, the cellular events preceding generation of protective immunity in humans are inadequately understood. We undertook an in-depth analysis of B cell and T cell immune responses to IIV in 35 healthy adults. Using recombinant hemagglutinin (rHA) probes to dissect the quantity, phenotype, and isotype of influenza-specific B cells against A/California09-H1N1, A/Switzerland-H3N2, and B/Phuket, we showed that vaccination induced a three-pronged B cell response comprising a transient $CXCR5^{-}CXCR3^{+}$ antibody-secreting B cell population, $CD21^{hi}CD27^{+}$ memory B cells, and $CD21^{lo}CD27^{+}$ B cells. Activation of circulating T_{FH} cells correlated with the development of both $CD21^{lo}$ and $CD21^{hi}$ memory B cells. However, preexisting antibodies could limit increases in serum antibody titers. IIV had no marked effect on $CD8^{+}$, mucosal-associated invariant T, γδ T, and natural killer cell activation. In addition, vaccine-induced B cells were not maintained in peripheral blood at 1 year after vaccination. We provide a dissection of rHA-specific B cells across seven human tissue compartments, showing that influenza-specific memory ($CD21^{hi}CD27^{+}$) B cells primarily reside within secondary lymphoid tissues and the lungs. Our study suggests that a rational design of universal vaccines needs to consider circulating T_{FH} cells, preexisting serological memory, and tissue compartmentalization for effective B cell immunity, as well as to improve targeting cellular T cell immunity.

INTRODUCTION

Influenza remains a significant public health problem, causing seasonal annual epidemics, occasional widespread pandemics, and sporadic high pathogenicity outbreaks in domestic animals. In humans, two influenza A virus (IAV) strains (H1N1 and H3N2) along with one influenza B virus (IBV), from either the Victoria and Yamagata lineage, co-circulate annually (*1*). Vaccination with an inactivated influenza virus is currently the most effective way of inducing strain-specific neutralizing antibodies directed against surface glycoproteins, hemagglutinin (HA) and neuraminidase (NA). In the absence of antibody-mediated immunity, preexisting memory B cells (*2*, *3*) and broadly cross-reactive memory T cells (*4*–*6*) can be recalled and protect against influenza. Because of the antigenic drift (accumulation of mutations in antigenic regions) of IAV and IBV, and antigenic shifts (generation of antigenically novel strains through recombination) of IAV, broadly cross-reactive memory B cell and T cell populations might be central for controlling antigenically distinct influenza strains. Thus, effective influenza vaccines need to establish long-lasting memory B cells and T cells, readily recalled during infection with novel influenza viruses.

After antigen reexposure, memory B cells develop into short-lived effectors [plasmablasts and plasma cells, jointly named as antibody-secreting cells (ASCs)] and rapidly provide antibodies. In addition, memory B cells reenter germinal centers, resulting in generation of affinity-matured long-lived plasma cells (LLPCs) and memory B cells (*7*, *8*). This process depends on costimulation and cytokine production by T follicular helper (T_{FH}) cells (*9*, *10*). After inactivated influenza vaccine (IIV), a transient population of ASCs, predominantly derived from memory B cells outside the germinal centers, emerges in peripheral blood on day 7 (d7) after vaccination and correlates with antibody titers (*2*, *11*). Concomitantly, a population of circulating T_{FH} (cT_{FH}; $CD4^{+}CXCR5^{+}$) cells (*12*) also emerges in peripheral blood on d7 after vaccination (*13*). These cT_{FH} cells exhibit a type 1 phenotype ($CXCR3^{+}CCR6^{-}$), express activation markers (ICOS and PD-1), provide help to memory (but not naïve) B cells for development into ASCs, and correlate with ASCs and antibody responses (*13*). However, the role of human cT_{FH} cells in establishing B cell memory is not entirely understood. Recent studies described new subsets of

[1]Department of Microbiology and Immunology, University of Melbourne, The Peter Doherty Institute for Infection and Immunity, Parkville, Victoria 3010, Australia. [2]World Health Organization (WHO) Collaborating Centre for Reference and Research on Influenza, The Peter Doherty Institute for Infection and Immunity, Melbourne, Victoria 3000, Australia. [3]Seqirus, 63 Poplar Road, Parkville, Victoria 3052, Australia. [4]Obstetrics, Nutrition and Endocrinology Group, Department of Obstetrics and Gynaecology, University of Melbourne, Mercy Hospital for Women, Heidelberg, Victoria 3084, Australia. [5]Immunology and Diabetes Unit, St Vincent's Institute of Medical Research, Fitzroy, Victoria 3065, Australia. [6]Lung Transplant Unit, Alfred Hospital, Melbourne, Victoria 3004, Australia. [7]Sydney Medical School, University of Sydney, Sydney, New South Wales 2006, Australia. [8]Chris O'Brien Lifehouse Cancer Centre, Royal Prince Alfred Hospital, Camperdown, New South Wales 2050, Australia. [9]Immunology Division, Garvan Institute of Medical Research, Darlinghurst, New South Wales 2010, Australia. [10]St Vincent's Clinical School, University of New South Wales, Sydney, New South Wales 2052, Australia. [11]Melbourne Sexual Health Centre and Department of Infectious Diseases, Alfred Hospital and Central Clinical School, Monash University, Melbourne, Victoria 3004, Australia. [12]ARC Centre for Excellence in Convergent Bio-Nano Science and Technology, University of Melbourne, Parkville, Victoria 3010, Australia.
*These authors contributed equally to this work.
†Corresponding author. Email: kkedz@unimelb.edu.au (K.K.); tho.nguyen@unimelb.edu.au (T.H.O.N.)

antigen-specific B cells, based on the expression of CD21 and CD71, emerging with variable dynamics after immunization (*14*, *15*). In addition, influenza exposure history and preexisting antibodies can shape the antibody response to IIV (*16*–*18*), although mechanisms are ill defined. Important questions remain with regard to the generation and maintenance of immune memory B cells and T cells after IIV.

Here, we dissected cellular events that precede the serological response to IIV as well as the tissue distribution of influenza-specific memory B cells across human tissues. These findings have fundamental implications for the rational design of vaccines that induce protective and long-lasting immunity against influenza viruses.

RESULTS

Influenza vaccination induces activation of cT_{FH} cells and expansion of $CXCR3^+CXCR5^-$ ASCs

To dissect the cellular events preceding generation of protective immunity to IIV, blood samples were obtained from healthy adults at baseline and on d7, d14, and d28 after intramuscular immunization. Our study involved 35 vaccinees aged 22 to 55 years old, over 3 years, with a total sample size of 42 (table S1). The vaccination history of the donors was unknown. A/California/7/2009 remained constant throughout 3 years of vaccination, whereas A/H3N2 and IBV components were updated annually to reflect antigenically drifted A/H3N2 strains and circulating Yamagata or Victoria IBV viruses (Fig. 1A).

The kinetics of cT_{FH} cells ($CD4^+CXCR5^+$) and ASCs ($CD19^+CD27^+CD38^{hi}$ B cells) in peripheral blood were evaluated (fig. S1). After vaccination, the numbers of cT_{FH} type 1 subset ($cT_{FH}1$; $CXCR3^+CCR6^-$) expressing ICOS and PD-1 ($ICOS^+PD\text{-}1^+cT_{FH}1$) significantly expanded ($P < 0.0001$) on d7, before returning to baseline by d14 (Fig. 1, B and C). The numbers of $cT_{FH}2$ ($CXCR3^-CCR6^-$) and $cT_{FH}17$ ($CXCR3^-CCR6^+$) cells did not increase after vaccination (fig. S2, A and B). We found increased ($P < 0.0001$) frequency of activated $CD38^{hi}$ cells within $ICOS^+PD\text{-}1^+cT_{FH}1$ set on d7 after vaccination (Fig. 1, D and E). Whereas CD38 expression was higher on $cT_{FH}2$ and $cT_{FH}17$ cells than on $cT_{FH}1$ cells at baseline ($P < 0.001$), $cT_{FH}1$ cells had a higher CD38 mean fluorescence intensity (MFI) at d7 ($P < 0.0001$) (fig. S2C). CD38 on d7 was higher on $ICOS^+PD\text{-}1^+cT_{FH}1$ cells than on nonactivated $ICOS^-PD\text{-}1^{+/-}cT_{FH}1$ cells ($P = 0.002$) (fig. S2D). These data show that vaccination with IIV specifically activates $cT_{FH}1$ cells.

As previously reported (*2*, *11*), ASCs transiently appeared in blood peaking on d7 after vaccination ($P < 0.0001$ compared to baseline) and then declining at d14 and d28 (Fig. 1, F and G). We found a transient increase in expression of CXCR3 on ASCs on d7 ($P < 0.001$) (Fig. 1, H and I), not observed on non-ASC ($non\text{-}CD38^{hi}CD27^+$) B cells ($P < 0.0001$) (Fig. 1J). In addition, although non-ASC B cells expressed CXCR5, circulating ASCs lacked CXCR5 expression ($P < 0.0001$) (Fig. 1K). Thus, circulating ASCs present in blood on d7 after vaccination display distinct expression patterns of chemokine receptors, CXCR3 and CXCR5, important for trafficking of B cells. Vaccination also increased serum antibody titers (d28 compared to baseline) against A/H1N1, A/H3N2, and IBV components (Fig. 1L), based on the HA inhibition assay (HAI). This assay measures serum antibodies that block the receptor binding on the HA head (but not binding to HA stem), irrespective of isotype. These data show that IIV induces transient and concurrent changes in circulatory B cell and T_{FH} compartments.

Recombinant HA probes detect influenza-specific B cells

To determine the quantity, phenotype, and isotype of B cells elicited by IIV, we identified influenza-specific B cells with recently developed recombinant HA (rHA) probes (*19*–*21*), consisting of four biotinylated trimeric rHA molecules conjugated to streptavidin-fluorochrome complexes. To prevent nonspecific binding to sialic acids on the cell surface, rHA probes contained mutations Y98F for IAV and T190G for IBV (*21*). We used rHA probes against three vaccine components: A/California/07/09-H1N1 (A/Cal09-H1), A/Switzerland/9715293/2013-H3N2 (A/Swi-H3), and B/Phuket/3073/2013 (BHA; Yamagata lineage) (Fig. 2A). Using peripheral blood mononuclear cells (PBMCs) from healthy adults, influenza probe–specific B cells were identified within mature class-switched $CD19^+CD3^-CD14^-CD16^-CD10^-IgD^-$ B cells, with exclusion of cells binding free fluorochrome-streptavidin (Fig. 2A and fig. S3).

We validated the specificity of rHA probes for detection of influenza-specific B cells using different experimental approaches (figs. S4 and S5). Dual rHA probe staining (two rHA probes of the same specificity conjugated to different fluorochromes) (*22*) showed that most of the class-switched IgD^- B cells were double-positive across allophycocyanin (APC)– and phycoerythrin (PE)–conjugated probes (97 and 90% for H1; 92 and 50% for H3; 91 and 86% for B; fig. S4, A and B), reflecting a high level of probe specificity. Because of its higher sensitivity, our subsequent data were generated using the H3-APC probe. However, double-positive rHA staining within unswitched IgD^+ B cells was considerably lower (17 to 55% depending on the probe and fluorochrome; fig. S4, A and B). Thus, we excluded them from our analyses because of high-level non–HA-specific rHA binding.

Then, we blocked rHA staining with sheep anti-HA sera against each of the probes. Blocking with cognate antisera specifically reduced rHA staining on class-switched B cells by 82 to 93% (fig. S4, C and D), further demonstrating specificity of rHA binding to IgD^- B cells.

We also single-cell FACS-sorted $CD19^+IgD^-IgM^-IgG^+CD27^+rHA^+$ B cells directly ex vivo from PBMCs on d28 after IIV. B cell receptor (BCR) heavy-chain sequences for $rHA\text{-}H1^+$ and $rHA\text{-}B^+$ B cells were recovered using a multiplex polymerase chain reaction approach (*23*). A high proportion of BCR sequences (57% for $rHA\text{-}H1^+$; 65% for $rHA\text{-}B^+$ B cells) exhibited clonal expansions (same IGHV usage and CDR3 homology) (fig. S5A), a reliable indicator of antigenic specificity. Furthermore, clonal sizes showed typical distributions of clones, with 1 to 2 largely expanded clones, 10 to 11 medium-sized clones, 16 to 23 smaller clones, and a natural tail of 83 to 97 singletons (fig. S5B). Because clonality is a function of sequencing depth, some of the singletons would also likely be HA-specific. In addition, our data show that the rHA-specific singletons use the same heavy-chain segments as the largely expanded clones (fig. S5C), suggesting their specificity.

At steady state, the numbers of peripheral blood $A/Cal09\text{-}H1^+$ B cells (median, 40.3 cells/ml blood) were significantly higher than $A/Swi\text{-}H3^+$ (median, 22.5 cells/ml blood; $P = 0.0028$) and $B/Phu\text{-}HA^+$ B cells (median, 24.2 cells/ml blood; $P = 0.0014$) (Fig. 2B). Influenza-specific B cells were grouped according to their isotype as IgG^+, IgA^+, and IgM^+ subsets (fig. S3). Although anti-IgA staining was not included because of the limited capacity of flow cytometry, our separate analysis showed that 100% ($n = 25$; fig. S6) of $A/Cal09\text{-}H1^+$ $IgG^-IgD^-IgM^-$ cells were IgA^+, and hence, $IgG^-IgD^-IgM^-$ cells were classified here as IgA^+. Whereas a larger proportion of $B/Phu\text{-}HA^+$ B cells were IgG^+ (median: H1, 74.2%; H3, 60.6%; B, 83.4%) (Fig. 2, C and D), in terms of numbers of B cells/ml, there were more

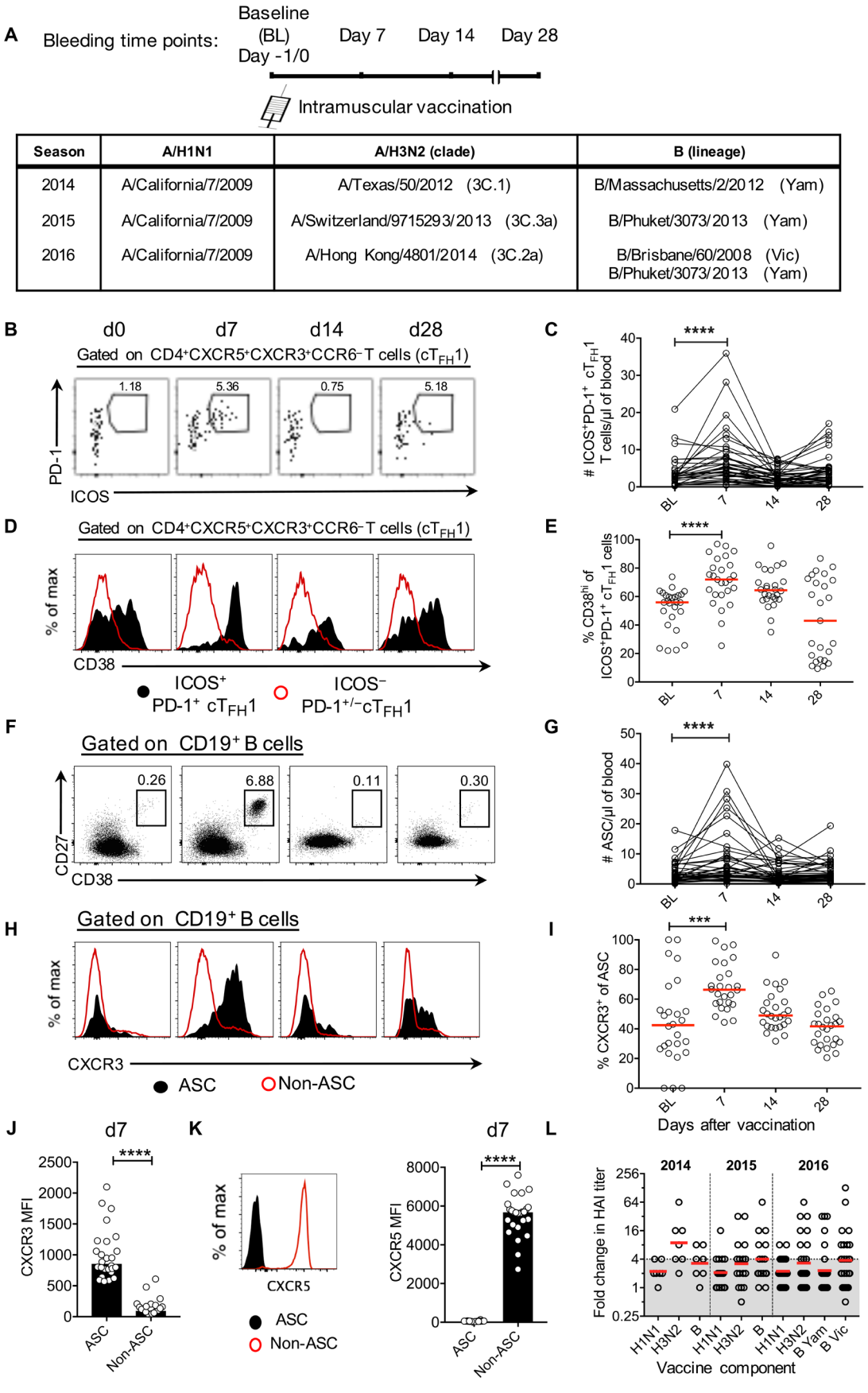

Season	A/H1N1	A/H3N2 (clade)	B (lineage)
2014	A/California/7/2009	A/Texas/50/2012 (3C.1)	B/Massachusetts/2/2012 (Yam)
2015	A/California/7/2009	A/Switzerland/9715293/2013 (3C.3a)	B/Phuket/3073/2013 (Yam)
2016	A/California/7/2009	A/Hong Kong/4801/2014 (3C.2a)	B/Brisbane/60/2008 (Vic) B/Phuket/3073/2013 (Yam)

Fig. 1. Vaccination induces activation of cT_{FH} cells and transient ASCs. (**A**) Study design and vaccine composition. Yam, Yamagata; Vic, Victoria. (**B**) Representative fluorescence-activated cell sorting (FACS) plots and (**C**) numbers of $ICOS^+PD\text{-}1^+cT_{FH}1$ cells after vaccination (n = 34 to 42). (**D**) CD38 expression on activated $cT_{FH}1$ cells. (**E**) Frequency of $CD38^{hi}$ cells in the $ICOS^+PD\text{-}1^+cT_{FH}1$ population (n = 26, 2016 cohort). (**F**) Representative FACS plots and (**G**) numbers of $CD27^{hi}CD38^{hi}$ASCs after vaccination (n = 42). (**H**) Expression of CXCR3 and (**I**) frequency of $CXCR3^+$ASCs after vaccination. (**J** and **K**) MFI of CXCR3 (J) and CXCR5 (K) expression on ASCs and non-ASCs at d7 (n = 26, 2016 cohort). (**L**) Serological response to vaccination, measured as fold change in HAI titers (2014, n = 7; 2015, n = 16; 2016, n = 26). Bars/lines indicate the median. Statistical significance from baseline or between groups was determined using Wilcoxon matched-pairs signed-rank test (**P < 0.005, ***P < 0.001, ****P < 0.0001).

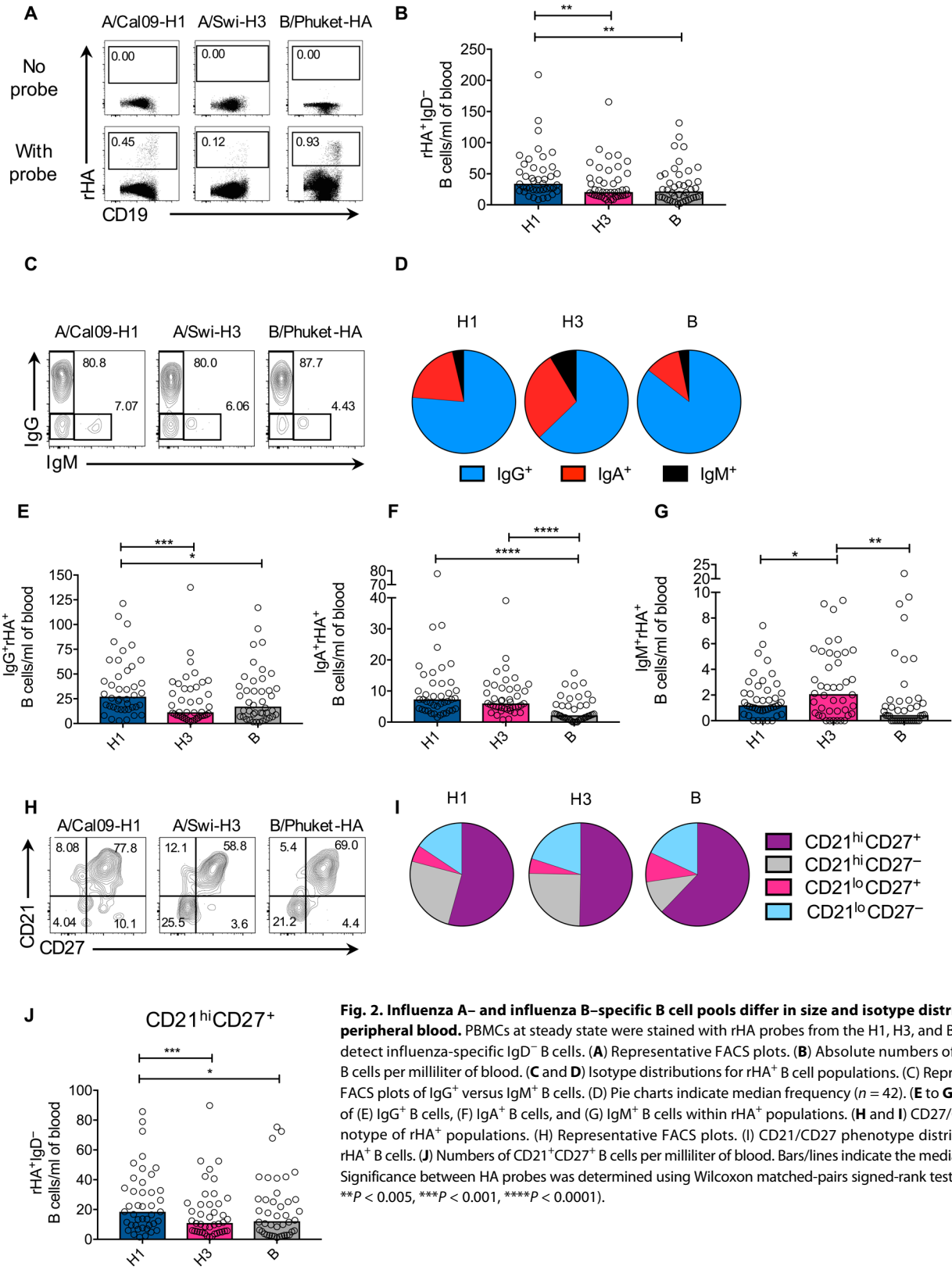

Fig. 2. Influenza A– and influenza B–specific B cell pools differ in size and isotype distribution in peripheral blood. PBMCs at steady state were stained with rHA probes from the H1, H3, and B viruses to detect influenza-specific IgD$^-$ B cells. (**A**) Representative FACS plots. (**B**) Absolute numbers of rHA$^+$IgD$^-$ B cells per milliliter of blood. (**C** and **D**) Isotype distributions for rHA$^+$ B cell populations. (C) Representative FACS plots of IgG$^+$ versus IgM$^+$ B cells. (D) Pie charts indicate median frequency ($n = 42$). (**E** to **G**) Numbers of (E) IgG$^+$ B cells, (F) IgA$^+$ B cells, and (G) IgM$^+$ B cells within rHA$^+$ populations. (**H** and **I**) CD27/CD21 phenotype of rHA$^+$ populations. (H) Representative FACS plots. (I) CD21/CD27 phenotype distributions of rHA$^+$ B cells. (**J**) Numbers of CD21$^+$CD27$^+$ B cells per milliliter of blood. Bars/lines indicate the median ($n = 42$). Significance between HA probes was determined using Wilcoxon matched-pairs signed-rank test (*$P < 0.05$, **$P < 0.005$, ***$P < 0.001$, ****$P < 0.0001$).

A/Cal09-H1$^+$ IgG$^+$ B cells (Fig. 2E). Accordingly, there were fewer IgA$^+$ or IgM$^+$ B/Phu-HA$^+$ B cells found than for the other two specificities. Analysis of the memory CD27 and activation CD21 (complement receptor 2) markers to identify resting memory B cells (CD21^{hi}CD27$^+$) (fig. S3) showed that the three rHA$^+$ populations exhibited similar phenotype distributions, with resting memory B cells being the most frequent (median: H1, 50%; H3, 48%; B, 55.2%) (Fig. 2, H and I). A/Cal09-H1$^+$ CD21^{hi}CD27$^+$ B cells were the most prominent (median: H1, 18.5 cells/ml; H3, 11 cells/ml; B, 12.2 cells/ml) (Fig. 2J), reflecting their greater abundance. Overall, although the IAV-H1$^+$ B cell pool is larger in size, the IBV-specific B cell pool contains relatively more IgG$^+$ B cells.

CD21^{hi}CD27$^+$ and CD21^{lo}CD27$^+$ influenza-specific B cells emerge in peripheral blood after vaccination

To determine how the rHA$^+$ B cell pool responds to IIV, we assessed numbers and phenotype of influenza-specific B cells after vaccination in the 2015 and 2016 cohorts. Whereas A/Cal09-H1 was constant across both years, the H3 component was updated in 2016 with the A/Hong Kong strain, belonging to the same clade (3C) but a different subclade (3C.2a) to the A/Switzerland strain (3C.3a). Because an A/Hong Kong rHA probe was unavailable, samples from the 2016 cohort were stained with the heterologous A/Swi-H3 probe. For IBV, the B/Phuket (Yamagata) strain was present in IIV in both years, as a sole IBV component in 2015, and together with the B/Brisbane (Victoria) in 2016 as a part of the quadrivalent formulation. B/Phuket-specific B cells were analyzed during 2015 and 2016, whereas a probe for B/Brisbane was unavailable.

Vaccination substantially increased the number of B cells specific for three IIV components ($P < 0.0001$) (Fig. 3, A and B). This increase was observed on d7, peaked at d14, and maintained until d28. Thus, IIV increases the size of the influenza-specific B cell pool, at least until d28 after immunization. For H3, HA-specific B cell patterns were similar when data were analyzed from both the 2015 cohort (using a homologous probe) and the 2016 cohort (using a heterologous probe) together (Fig. 3B) or separately (fig. S7), reflecting the effect of back-boosting and recall of memory B cells. In addition, a subset of B cells specific for each of the vaccine components transiently acquired an ASC-like phenotype (CD27^{hi}CD20^{lo}) on d7 (Fig. 3, C and D). After vaccination, IgG$^+$, IgA$^+$, and IgM$^+$ influenza-specific B cells underwent significant expansion (Fig. 3E). The response was mainly dominated by IgG$^+$ B cells, with a median of 63.7 A/Cal09-H1$^+$ cells/ml, 36.7 A/Swi-H3$^+$ cells/ml, and 24.2 BHA$^+$ cells/ml of blood on d14 and a smaller IgA$^+$ population (14.9 A/Cal09-H1$^+$ cells/ml, 12.5 A/Swi-H3$^+$ cells/ml, and 7.9 BHA$^+$ cells/ml). Although minimal, significant changes were observed for IgM$^+$rHA$^+$ B cells ($P < 0.05$). To confirm the data obtained by rHA staining, we used polyclonal stimulation (CpG, CD40L, and IL-21) and a B cell enzyme-linked immunospot (ELISPOT) assay (fig. S8). Although at baseline B cells against A/Cal09 H1 and B/Phu were undetectable, B cells against both strains increased at d14 (fig. S8A), similarly to measurements by FACS (fig. S8B). The number of IgG$^+$rHA$^+$ B cells correlated ($r_s = 0.7$, $P = 0.0005$) with the number of IgG$^+$ spot-forming units (SFU/million PBMCs) (pooled data for H1 and B from d0 and d14), supporting our analysis by rHA probes.

Further phenotyping of rHA$^+$IgG$^+$ B cells revealed that although these cells predominantly displayed a resting memory phenotype (CD21^{hi}CD27$^+$) at baseline, HA-specific B cells across all vaccine components transitioned to an activated memory phenotype (CD21^{lo}CD27$^+$) from d7 until d28, with a noticeable peak on d14 (Fig. 3, F and G). The CD21^{lo} B cell population was distinct from the ASC phenotype because the latter cells were CD20^{lo} (fig. S9). Overall, IIV increased the numbers in the CD21^{hi} and CD21^{lo} IgG$^+$ influenza-specific B cell pool, both of which peaked on d14 for IgG$^+$ B cells.

Activation of cT$_{FH}$1 cells correlates with increased numbers of CD21^{hi}CD27$^+$ and CD21^{lo}CD27$^+$ HA-specific B cells in the periphery

We found four key effector cells in the immune response to IIV: ASCs and activated cT$_{FH}$1 cells, transiently emerging in the circulation on d7, and CD21^{hi}CD27$^+$ and CD21^{lo}CD27$^+$ influenza-specific B cells, peaking on d14. We further investigated how these cellular events are connected and how they relate to the magnitude of the serological response. Because the 2016 vaccine formulation included a new H3N2 strain and a second IBV strain, for which rHA$^+$ probes were unavailable, the analysis focused on the 2015 cohort ($n = 16$). For other analyses, pooled data from the 2015 and 2016 cohorts ($n = 42$) were used.

A correlation between the number of blood ASCs per microliter on d7 and the antibody response after IIV (total fold change on d28 over d0) ($r_s = 0.37$, $P = 0.013$) was found (Fig. 4A). The total fold increase was defined as the sum of the fold change for all the vaccine components, because the cT$_{FH}$1 and ASCs detected on d7 could not be attributed to a specific vaccine component. Accordingly, individuals who seroconverted after IIV (≥4-fold change in HAI titers to at least one vaccine component) had a significantly higher ASC/μl numbers at d7, as compared to nonseroconverters ($P = 0.0381$) (Fig. 4B), as in studies showing that the serological response to vaccination was linked to the emergence of ASCs (*2*, *24*). In the 2014 cohort with longitudinal serum samples, the HAI titer increased as early as d7 (Fig. 4C), suggesting that the serological response observed after vaccination is derived from this transient ASC population.

Similarly, ICOS$^+$PD-1$^+$cT$_{FH}$1 cells showed a moderate correlation with the total fold increase in HAI titers ($r_s = 0.43$, $P = 0.0042$) (Fig. 4D). Notably, seroconverters had a higher number of ICOS$^+$PD-1$^+$cT$_{FH}$1 cells when compared to nonseroconverters ($P = 0.0328$) (Fig. 4E). In addition, the number of ASCs on d7 showed a moderate positive correlation with the number of ICOS$^+$PD-1$^+$cT$_{FH}$1 cells on d7 ($r_s = 0.6307$, $P < 0.0001$) (Fig. 4F). Furthermore, the number of ICOS$^+$PD-1$^+$cT$_{FH}$1 cells on d7 also correlated with the fold change in both CD21^{hi}CD27$^+$ ($r_s = 0.7353$, $P = 0.0017$) and CD21^{lo}CD27$^+$ IgG$^+$ memory B cells specific for all vaccine components ($r_s = 0.7265$, $P = 0.002$) (Fig. 4G), highlighting a central role for cT$_{FH}$1 cells in B cell memory generation and seroconversion. Thus, the emergence of cT$_{FH}$1 cells is important for the immune response to IIV because they are linked to the increase of ASCs and CD21^{hi}CD27$^+$ and CD21^{lo}CD27$^+$ HA-specific B cell memory in the periphery.

Preexisting antibodies negatively correlate with the serological response and the emergence of CD21^{lo}CD27$^+$ influenza-specific B cells

Individuals who seroconverted to H1 and B had lower serum titers at baseline than those who did not respond to the vaccine (H1: $P = 0.0062$; B: $P = 0.0045$) (Fig. 5A), showing that seroconversion is influenced by preexisting serum titers, as reported (*17*). This was not observed for H3N2 ($P = 0.29$), which differed in both 2015 and 2016. Correspondingly, preexisting titers to H1 and B components showed a negative correlation with the cognate fold increase in HAI titers

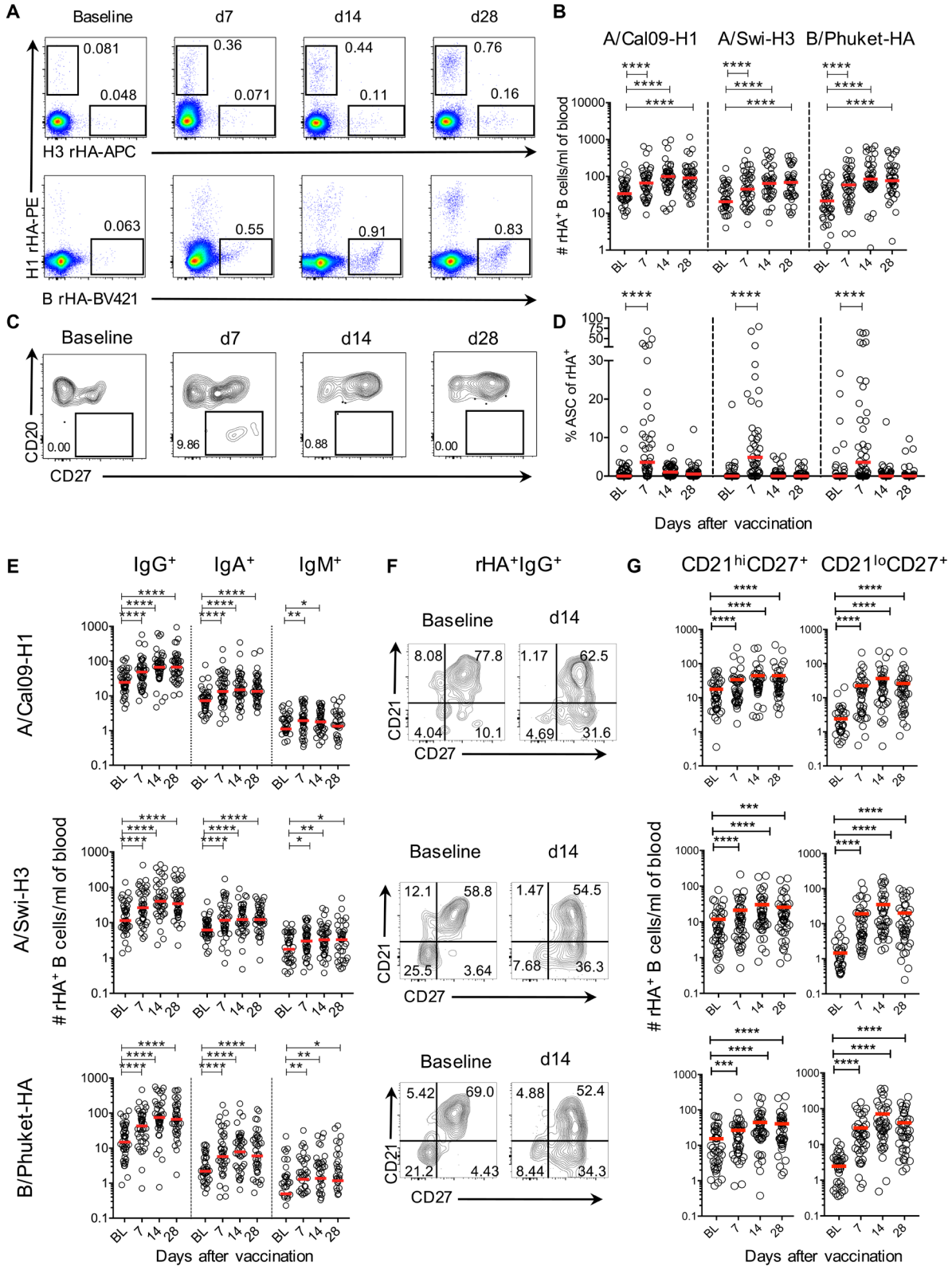

Fig. 3. IIV induces CD21^{hi}CD27^{+} and CD21^{lo}CD27^{+} influenza-specific B cells. (**A**) Numbers of rHA^{+}IgD^{-} B cells before and after vaccination. Representative FACS plots of rHA^{+} B cells after vaccination. (**B**) Numbers of rHA^{+} B cells per milliliter of blood for each vaccine component. (**C**) Representative FACS plots and (**D**) frequency of CD27^{+}CD20^{-}rHA^{+} B cells before and after vaccination. (**E**) Numbers of isotype-specific rHA^{+} B cells. (**F**) Representative FACS plots for d0 and d14. (**G**) Numbers of CD21^{hi}CD27^{+} and CD21^{lo}CD27^{+} IgG^{+}rHA^{+} B cells. (E and G) Pooled data from 2015 and 2016 cohorts ($n = 42$). Bars indicate the median. Statistical significance for changes from baseline was determined using Wilcoxon matched-pairs signed-rank test (*$P < 0.05$, **$P < 0.005$, ***$P < 0.001$, ****$P < 0.0001$).

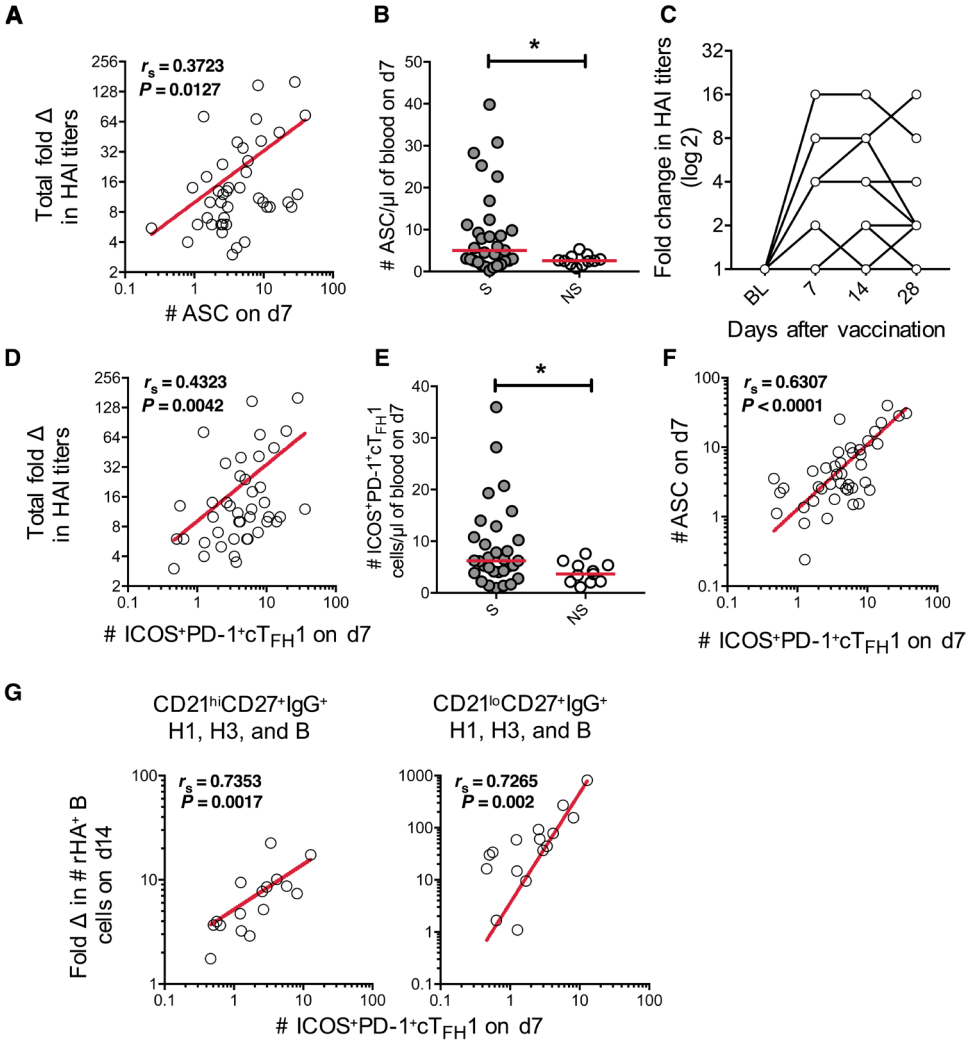

Fig. 4. $cT_{FH}1$ cells correlate with a boosting of influenza-specific memory B cells. (**A**) Correlation between d7 ASCs and total fold change (Δ) (sum of vaccine response to vaccine components) in serum titers after vaccination. (**B**) Numbers of ASC on d7 in seroconverters (S) ($n = 19$) and nonseroconverters (NS) ($n = 7$). (**C**) Fold change on d28 over baseline in HAI serum titers from pooled data, from three vaccine components of the 2014 cohort ($n = 7$), at different time points. (**D**) Correlation between d7 $ICOS^+PD\text{-}1^+cT_{FH}1$ cells and fold change in serum titers after vaccination. (**E**) Numbers of $ICOS^+PD\text{-}1^+cT_{FH}1$ cells on d7 in seroconverters and nonseroconverters. (**F**) Correlation between d7 ASCs and $ICOS^+PD\text{-}1^+cT_{FH}1$ cells. (**G**) Correlation between fold changes in $CD21^{hi}CD27^+$ B cells or $CD21^{lo}CD27^+$ B cells on d14 and numbers of $ICOS^+PD\text{-}1^+cT_{FH}1$ on d7. (A, D, and F) Data from 2015 and 2016 cohorts ($n = 42$). (G) Data from 2015 cohort ($n = 16$). (A, D, and F to I) Correlation was assessed using Spearman's correlation coefficient (r_s). (B and E) Bars indicate the median. Statistical significance was determined using the Mann-Whitney test (*$P < 0.05$).

(H1: $r_s = -0.5$, $P = 0.001$; B: $r_s = -0.55$, $P = 0.0001$) (Fig. 5B). This differed for the drifted H3 component ($r_s = -0.29$, $P = 0.06$). When HAI titers against all vaccine components were added, there was a significantly strong negative correlation between the baseline HAI titers and the fold increase in HAI titers on d28/d0 ($r_s = -0.56$, $P = 0.0001$) (Fig. 5C).

Conversely, the total preexisting serum titers on d0 did not affect the emergence of total ASCs ($r_s = 0.063$, $P = 0.69$) (Fig. 5D) or $ICOS^+PD\text{-}1^+cT_{FH}1$ cells ($r_s = -0.02571$, $P = 0.8716$) (Fig. 5E) at d7. In addition, preexisting serum titers had no effect on the fold change of memory $CD21^{hi}rHA^+$ B cells for either of the components (H1: $r_s = -0.16$, $P = 0.54$; B: $r_s = -0.12$, $P = 0.67$; H3: $r_s = 0.08$, $P = 0.76$) (Fig. 5F). However, preexisting titers against B, but not H1 or H3, negatively correlated with the fold change of cognate $CD21^{lo}rHA^+$ B cells (H1: $r_s = -0.35$, $P = 0.2$; B: $r_s = -0.76$, $P = 0.0015$; H3: $r_s = -0.0045$, $P = 0.992$) (Fig. 5G). Thus, preexisting serological memory can limit seroconversion and the magnitude of $CD21^{lo}$ B cells.

Vaccination with IIV does not induce $CD8^+$ and innate T cells

To determine the effect of IIV on cellular immunity other than cT_{FH} cells, we examined influenza-specific $CD8^+$ T cells, $CD4^+$ T cells, γδ T cells, mucosal-associated invariant T (MAIT) cells, and natural killer (NK) cells, assessed by intracellular cytokine staining (ICS) for interferon-γ (IFN-γ) and tumor necrosis factor (TNF) after an ex vivo overnight stimulation with IAV and IBV (A/Cal09 H1N1pdm09, B/Phuket) in seven donors vaccinated in 2015 (fig. S10). The frequency and numbers of IFN-γ^+CD8^+ T cells, γδ T cells, MAIT cells, and NK cells remained unchanged in response to IAV and IBV, with no apparent differences between the pre- and post-vaccination time points (Fig. 6, A and B, and fig. S11). Consistent with previous studies, IFN-γ^+CD4^+ T cells increased in response to IAV (not IBV) at d14 (median: d0, 819 cells/ml blood; d14, 1129 cells/ml blood; $P = 0.038$), although this increase was not maintained at d28. To further probe any effects of IIV on $CD8^+$ T cells, we used fluorochrome-conjugated peptide/major histocompatibility complex–I (MHC-I) tetramers for IAV-derived epitopes [A2-$M1_{58-66}$, A1-NP_{44-52}, and B8-$NP_{225-233}$, depending on the donor's human leukocyte antigens (HLAs)] in three donors (fig. S12). Consistent with the ICS, vaccination did not alter the frequencies (Fig. 6, C and D) or differentiation status (CD27/CD45RA phenotype) (Fig. 6, E and F) of tetramer$^+CD8^+$ T cells. Last, there were no differences in the expression of differentiation (CD27/CD45RA), activation (HLA-DR/CD38), or proliferation (Ki-67) markers (Fig. 6G) or the effector granzyme B on T cells ($n = 14$) (fig. S12). Overall, influenza-specific T cell compartments in the circulation (with the exception of $CD4^+$ T cells) remain unchanged after IIV.

Vaccine-induced memory B cells are not maintained in peripheral blood

For vaccine-induced immunity to be protective, it needs to be long-lived. We assessed the longevity of vaccine-induced influenza-specific

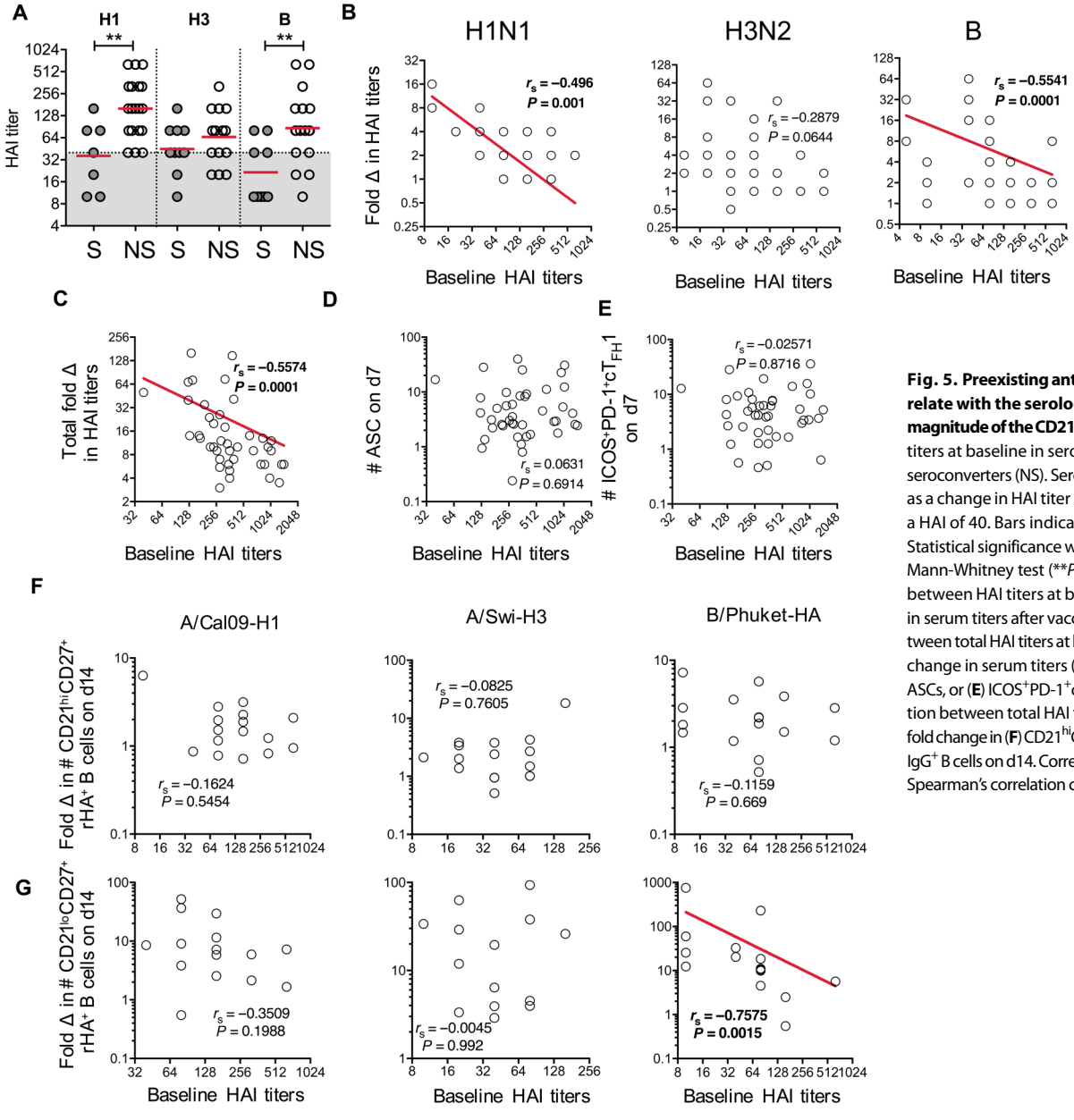

Fig. 5. Preexisting antibodies negatively correlate with the serological response and the magnitude of the CD21^{lo} B cell response. (**A**) HAI titers at baseline in seroconverters (S) and non-seroconverters (NS). Seroconversion was defined as a change in HAI titer ≥4. Dotted line indicates a HAI of 40. Bars indicate the geometric mean. Statistical significance was determined using the Mann-Whitney test (**$P < 0.005$). (**B**) Correlation between HAI titers at baseline and fold change in serum titers after vaccination. Correlations between total HAI titers at baseline and (**C**) total fold change in serum titers (d28/d0), (**D**) numbers of ASCs, or (**E**) ICOS$^+$PD-1$^+$cT$_{FH}$1 cells on d7. Correlation between total HAI titers at baseline and the fold change in (**F**) CD21^{hi}CD27$^+$ or (**G**) CD21^{lo}CD27$^+$ IgG$^+$ B cells on d14. Correlation was assessed using Spearman's correlation coefficient (r_s).

antibodies and B cells. Serum titers (but not influenza-specific B cells) for the three vaccine components were stable (within the fourfold difference) over the 1-year period (>350 days) after vaccination (Fig. 7, A and B). However, when the isotype distributions for vaccine components were analyzed, a loss of vaccine-induced IgG$^+$ and IgA$^+$ rHA$^+$ B cells was observed at 1 year (Fig. 7, C and D). This loss was pronounced and significant ($P < 0.05$) when IgG$^+$CD21^{hi} and IgG$^+$CD21^{lo} rHA$^+$ B cells were analyzed (Fig. 7E), suggesting that the vaccine-induced influenza-specific memory B cells are not maintained in peripheral blood.

Because eight individuals received IIV vaccination in two consecutive years, we analyzed rHA$^+$IgD$^-$ B cells within these individuals across different years. Overall, total IgD$^-$rHA$^+$, CD21^{hi} rHA$^+$, or CD21^{lo}rHA$^+$ B cell responses were comparable across repeated vaccinations (Fig. 7, F and G). However, when the fold change over its respective baseline for each year was calculated, B cell responses were significantly larger on d7 ($P < 0.05$) in the second year for total rHA$^+$ B cells and for IgG$^+$CD21^{hi} rHA$^+$ B cells (fig. S13). Although these findings are interesting, the small number of donors and the lack of a vaccination history precluded us from further dissecting the effects of previous vaccination on influenza-specific B cell responses.

B cells show distinct patterns of tissue compartmentalization

Because the loss of vaccine-induced B cell memory in blood could result from transition between phenotypes, contraction of vaccine-induced B cell pools, or migration of memory B cells into tissues, we analyzed the distribution and phenotype of total and influenza-specific B cells across seven human tissue compartments. Spleens, lungs, and lymph nodes were obtained from deceased organ donors,

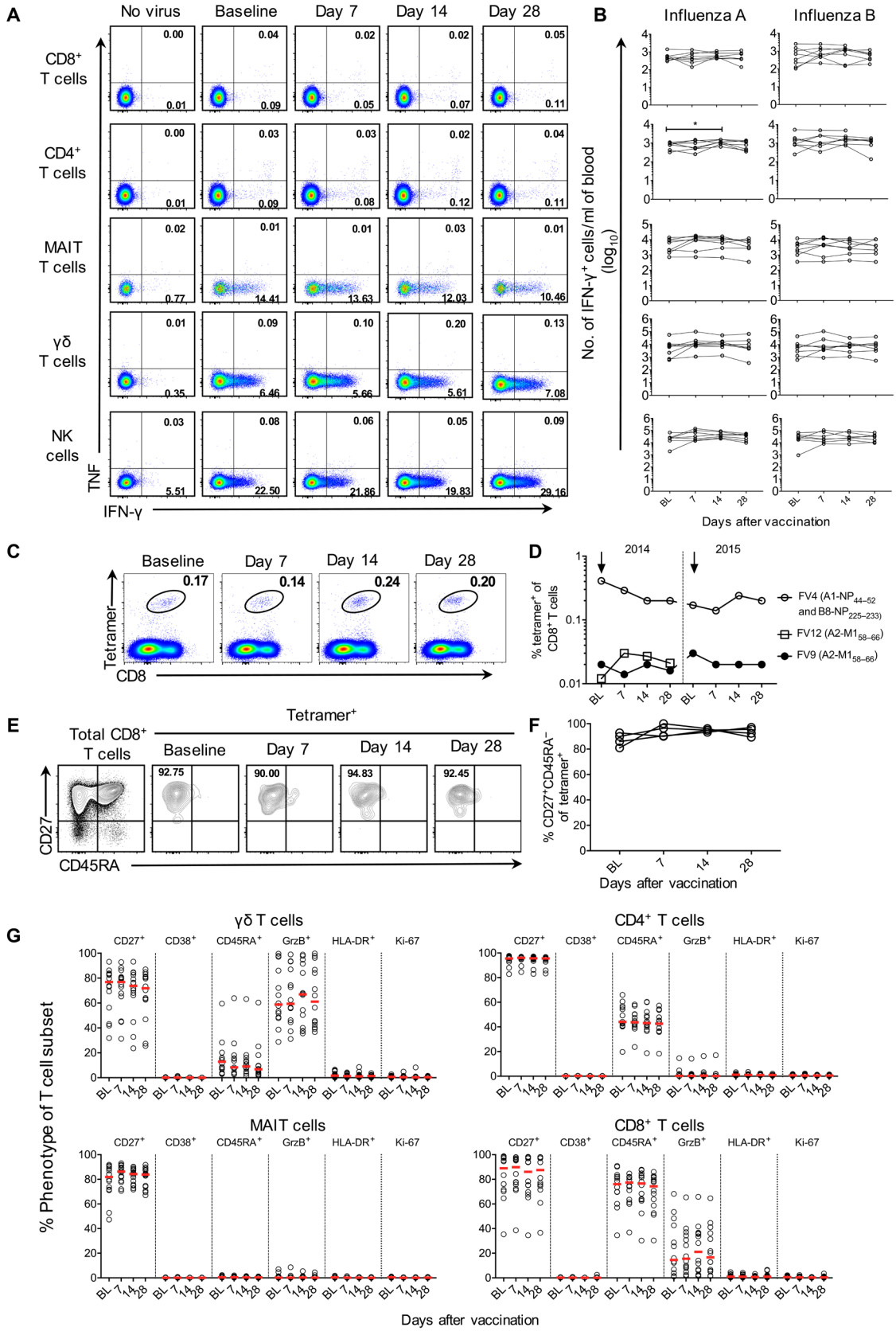

Fig. 6. Vaccination fails to induce CD8$^+$ and innate T cell responses. (**A** and **B**) IFN-γ/TNF production after overnight stimulation with live IAV-H1N1 or IBV-B/Phuket. (A) Representative FACS plots of H1N1 stimulation. (B) Numbers of IFN-γ$^+$ cells per milliliter of blood after IAV or IBV stimulation (n = 7, 2015 cohort). "No virus" control counts were subtracted. Significance for changes between time points was determined using the Friedman test (*P < 0.05). (**C**) IAV-specific CD8$^+$ T cells were detected by peptide/MHC-I tetramers (A2-M1$_{58–66}$, A1-NP$_{44–52}$, and B8-NP$_{225–233}$). FACS plots are gated on CD3$^+$ cells, and percentages are based on CD8$^+$ T cells. (**D**) Longitudinal tracking of % tetramer$^+$CD8$^+$ T cells (n = 3). Arrows indicate vaccination. (**E**) FACS plots of CD27/CD45RA expression on tetramer$^+$CD8$^+$ T cells. (**F**) Longitudinal tracking of activated CD27$^+$CD45RA$^-$tetramer$^+$CD8$^+$ T cells (n = 3). (**G**) T cell subsets were assessed for activation and differentiation markers. Bars indicate the median. Data are from randomly selected donors (n = 14, 2014 to 2015 cohorts).

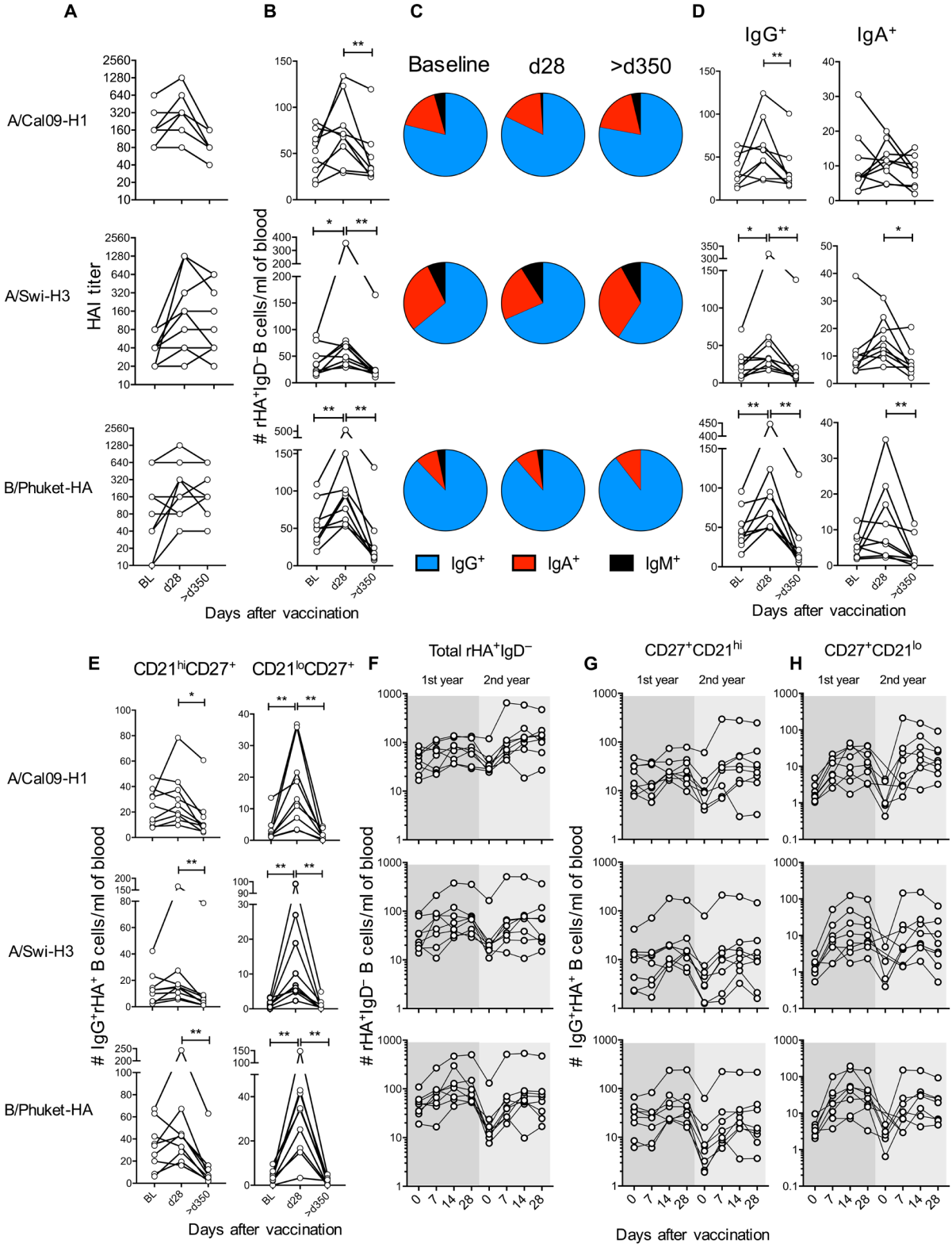

Fig. 7. Vaccine-induced influenza-specific B cells are not maintained in peripheral blood. Responses in (**A**) antibody serum titers, (**B**) numbers of IgD$^-$rHA$^+$ B cells, (**C**) pie graphs of isotype distribution within each rHA$^+$ population, (**D**) changes in isotype-specific class-switched rHA$^+$ B cells, and (**E**) numbers of CD21^{hi} and CD21^{lo} influenza-specific B cells at baseline, d28, and >d350 (n = 9, 2015 cohort). Significance for changes from baseline was determined using Wilcoxon matched-pairs signed-rank test (*P < 0.05, **P < 0.005). (**F** to **H**) Numbers of (F) total IgD$^-$rHA$^+$ B cells and (G) CD21^{hi} and (H) CD21^{lo}IgG$^+$rHA$^+$ B cells in individuals vaccinated in 2015 and 2016 (n = 8).

whereas peripheral blood, bone marrow, cord blood, and tonsils were obtained from healthy individuals. B cells were phenotypically divided into four populations based on the expression of CD27 and CD21. Naïve B cells were defined as $CD21^{hi}CD27^{-}$, resting memory as $CD21^{hi}CD27^{+}$, activated memory as $CD21^{lo}CD27^{+}$, and tissue-like (atypical) memory as $CD21^{lo}CD27^{-}$. Dual rHA probe staining confirmed the probe specificity in tissues (spleen and lung), as most of the $rHA^{+}IgD^{-}$ B cells were double-positive (91%/71% for H1; 93%/71% for H3; across APC/PE-conjugated probes; fig. S14, A and B).

Total mature $CD19^{+}CD3^{-}CD14^{-}CD16^{-}CD10^{-}$ B cells were enriched in secondary lymphoid organs (SLOs), with a median of ~50% lymphocytes being B cells in the tonsils, lymph nodes, and spleen, as compared to 6.5% in adult blood, 13.7% in cord blood, 11.1% in bone marrow, and 4.8% in the lung (Fig. 8A). Naïve B cells ($CD21^{hi}CD27^{-}$) were found in human tissues, alongside the other B cell subsets (Fig. 8B). Most of the naïve B cells were detected in cord blood (86.4%) and bone marrow (88.3%), consistent with the lack of antigen exposure in cord blood and the development of B cells in the bone marrow. About 75% of blood and tonsil B cells were unswitched, whereas the spleen and lymph nodes contained a higher proportion of resting memory B cells (48.2 and 63.3%). The human lung contained 58% resting memory B cells and 38.6% unswitched B cells. Activated memory ($CD21^{lo}CD27^{+}$) B cells were infrequent, consistent with the donors' healthy status. Similar results were obtained from isotype analysis across human tissues (Fig. 8C). $IgD^{+}IgM^{+}$ B cells were the predominant subset across tissues, followed by $IgD^{+}M^{-}$ B cells and then class-switched B cells (IgG^{+}, IgA^{+}, IgM^{+}). IgA^{+} and IgM^{+} B cells were most prevalent in the lymph node, spleen, and lung.

Influenza-specific class-switched B cells (A/Cal09-$H1^{+}$, A/Swi-$H3^{+}$) were readily detected in all tissues (Fig. 8D). The frequency of rHA^{+} B cells ranged from 0.029 to 0.4% of IgD^{-} B cells. Furthermore, although the frequency of $rHA^{+}IgD^{-}$ cells within B cells was similar across tissues, $rHA^{+}IgD^{-}$ B cells within lymphocytes were more abundant in SLOs (tonsils, lymph nodes, and spleen) than in other tissues. Whereas in blood only 39.8% of $rHA^{+}IgD^{-}$ B cells were $CD27^{+}CD21^{hi}$, there was an enrichment of $CD27^{+}CD21^{hi}rHA^{+}$ B cells in all tissues (mean, 80.9 to 98%) (Fig. 8E). Although $IgG^{+}rHA^{+}$ B cells were more prominent in the circulation (mean, 87.9%), this was lower in tissues (50.4 to 70.9%). Instead, tissues showed larger proportions of IgM^{+} and IgA^{+} rHA^{+} B cells (Fig. 8F). Overall, influenza-specific B cell memory is enriched outside of peripheral blood.

To normalize for differences between donors due to exposure history and age, we analyzed B cell tissue compartmentalization in paired peripheral blood and spleen samples (n = 5; table S2). Analysis of total B cells confirmed enrichment of $CD21^{hi}CD27^{+}$ memory in the spleen compared to blood (Fig. 8H) and differential distribution of different isotypes between blood and tissues (fig. S15). Because of the low cell numbers available, we could not confidently detect influenza-specific B cells.

DISCUSSION

Vaccination with inactivated influenza remains the predominant prophylactic measure against infection. Understanding the cellular events that precede the induction of protective immunity is pivotal in the development of better vaccines. We provide a comprehensive analysis of the immune response to vaccination in healthy individuals. Using rHA probes to characterize influenza-specific B cells, we show that vaccination induces an early wave of influenza-specific short-lived effectors (ASCs), accompanied by an increase in antibody titers, and a second wave of $CD21^{hi}CD27^{+}$ and $CD21^{lo}CD27^{+}$ B cells. Concomitantly, activated $cT_{FH}1$ cells correlated with all arms of this response. Vaccine-induced B cells were not maintained in peripheral blood, and overall, human memory B cells were enriched in SLOs and peripheral tissues. Vaccination had no impact on $CD8^{+}$ and innate T cells. Our analysis is based on a limited number of vaccinees, with unknown and variable infection and vaccination history. In addition, our serological analysis by HAI only measures antibodies that block the receptor binding site but not the broadly cross-reactive anti-HA stem antibodies and does not distinguish between isotypes. Nonetheless, our study provides insights into the human B cell response and recapitulates fundamental aspects of B cell biology from animals, translating them into humans across different tissues.

Previously, ASCs on d7 correlated with seroconversion (*2*, *24*). Our kinetic data and correlation analyses support this model. Consistent with studies in mice (*25*, *26*) and tetanus vaccination in humans (*27*), our findings show that the emergence of ASCs is accompanied by a chemotactic switch, specifically the loss of CXCR5, releasing B cells from germinal centers and preventing their reentry, and up-regulation of CXCR3, directing them to sites of inflammation and likely the bone marrow (*28*). The $CD21^{hi}CD27^{+}$ population represents a resting B cell memory population. These memory cells were detected in blood at steady state and in tissues, with their numbers being transiently boosted by vaccination. Activated memory $CD21^{lo}CD27^{+}$ B cells are distinct from ASCs because they express CD20. These cells were detectable at steady state in blood and tissues but emerged after vaccination. The fate of each population remains unclear, with both $CD21^{hi}$ and $CD21^{lo}$ cells persisting for at least 4 weeks, but subsiding by 1 year after vaccination.

Recent reports described human antigen-specific B cells with low CD21 expression. A newly described B cell phenotype ($CD38^{lo/int}CD20^{hi}CD27^{+}CD71^{+}$), termed activated B cells (ABCs), peaks on d14. On the basis of clonal relationships, ABCs from d7 eventually develop into memory B cells (*14*). $CD21^{lo}$ B cells ($CD38^{lo}CD21^{lo}CD27^{+}$), which emerge on d14 after IIV, are enriched within influenza-specific B cells, express transcriptional programs associated with plasma cell differentiation, and are identified as recent emigrants of germinal centers, suggesting that they might be precursors of LLPCs (*15*). Although we did not measure CD38 or CD71 expression on rHA^{+} B cells, a large population of $CD21^{lo}CD27^{+}CD20^{hi}$ influenza-specific B cells was induced by vaccination and with different dynamics to the ASCs.

Since the initial description of circulating $CXCR5^{+}CD4^{+}$ T cells as counterparts of T_{FH} cells in blood, their role in regulating vaccine responses is known (*12*, *13*). Seminal studies showed that specialization occurs between different cT_{FH} subsets and their ability to stimulate naïve or memory B cells to differentiate into ASCs (*12*, *13*). In that regard, $cT_{FH}1$ cells have a prominent role in facilitating seroconversion after vaccination, which is predominantly memory-derived (*2*, *11*). However, on the basis of current data, the role of cT_{FH} cells during IIV is limited to the interplay with serum antibodies. We show that activation of $cT_{FH}1$ cells on d7 correlates with emergence of $CD21^{hi}CD27^{+}$ and $CD21^{lo}CD27^{+}$ influenza-specific B cells on d14 after vaccination, implicating $cT_{FH}1$ cells as key players in the establishment of influenza-specific B cell memory. Recently, T cell receptor repertoire analysis of cT_{FH} cells after repeated IIV vaccination revealed the recruitment of recurrent clones (*29*), providing evidence that activated cT_{FH} cells are recalled from resting memory pools.

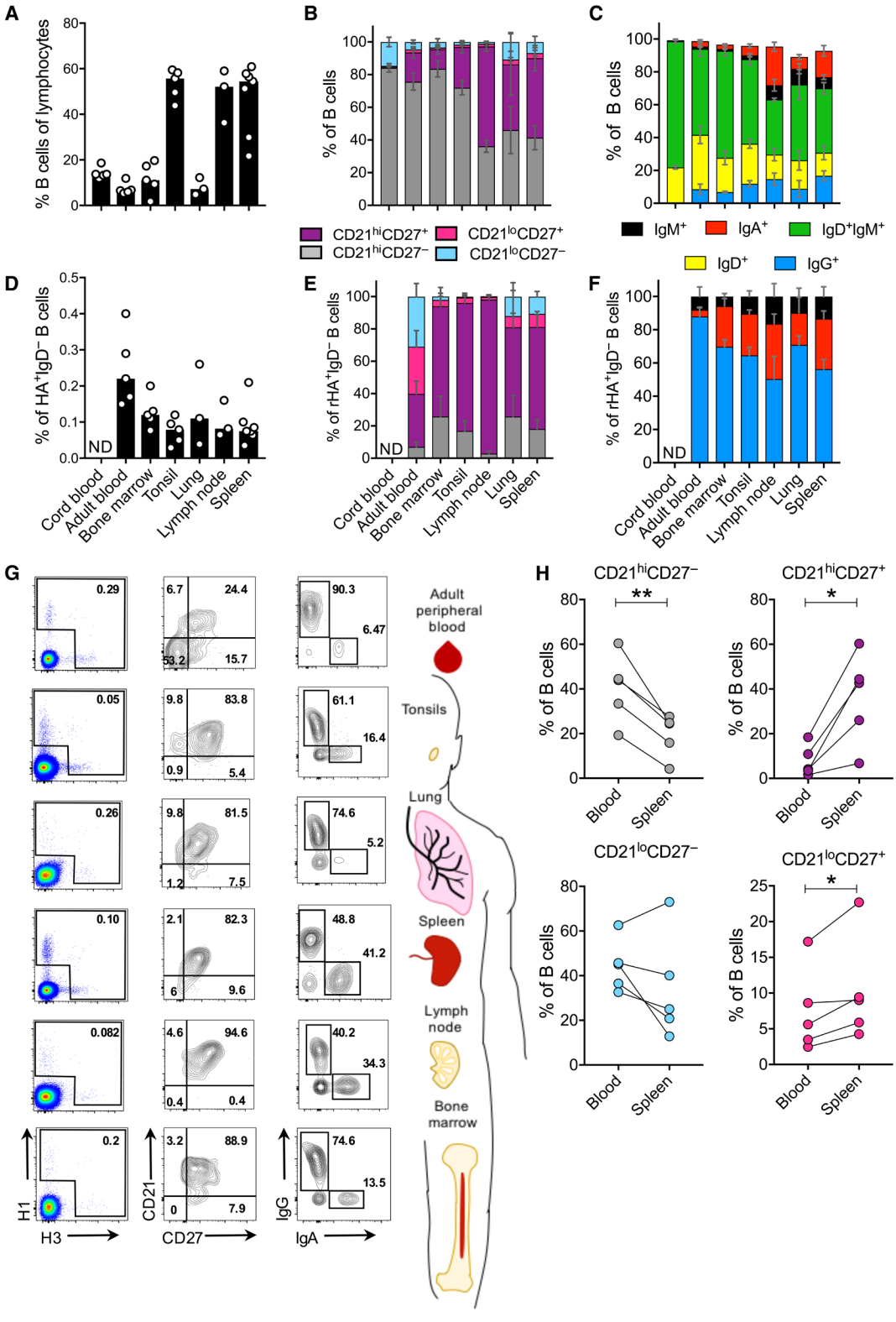

Fig. 8. Influenza-specific B cells show distinct patterns of tissue compartmentalization. (**A**) Frequency of $CD19^+CD10^-$ B cells across human tissues. (**B**) CD21/CD27 phenotype and (**C**) isotype of B cells across tissues. (**D**) Frequency of rHA^+ (H1/H3) IgD^- B cells across tissues. (**E**) Phenotype distribution and (**F**) isotype distribution of rHA^+ B cells across tissues. For isotype distributions, the frequency of each isotype was normalized to the sum of all three isotypes. (**G**) Representative FACS plots are shown. (A and D) Bars indicate median. (B, C, E, and F) Lines indicate mean, and error bars show SEM. Adult blood, $n = 5$; cord blood, $n = 5$; bone marrow, $n = 5$; tonsil, $n = 5$; lymph node, $n = 3$; lung, $n = 3$; spleen, $n = 7$. (**H**) PBMCs from paired blood and spleen samples were analyzed. Frequency of each CD21/CD27 population within total B cells for each blood and spleen pair ($n = 5$) is shown. Significance was assessed using a paired *t* test (*$P < 0.05$; **$P < 0.005$). ND, not determined.

Preexisting serological memory affected the magnitude of the serological response, and individuals who did not seroconvert had higher HAI titers at baseline than seroconverters, consistent with previous observations (*17*, *30*). The mechanism is unclear, but others suggested that preexisting antibodies mask or block antigenic epitopes on HA and/or induce the formation of immune complexes, which could aid antigen clearance, thus limiting the B cell response (*17*, *31*). We found an effect of serum titers at baseline on the magnitude of $CD21^{lo}$

B cells on d14, although this was only observed for IBV. It is also possible, however, that seroconversion (fourfold change in titers) is harder to detect in individuals with preexisting high titers.

Despite the substantial effects of IIV on the B cell and $CD4^+/T_{FH}$ compartments, other T cell populations were apparently unaffected. Specifically, IAV- and IBV-specific $CD8^+$ T cells were unaffected in frequency and phenotype. Whether this is due to antigen content, inadequate inflammation, or lack of cross-presentation in the absence of viral replication is unclear. Given the prominent role of $CD8^+$ T cells in cross-protective immunity (*4*–*6*), even against antigenically shifted strains like avian H5N1 (*32*) and H7N9 (*6*, *33*), vaccines that establish $CD8^+$ T cells are of considerable importance.

Although vaccination induced robust humoral immunity, the B cell response was not maintained in peripheral blood over time. This likely reflects the expected contraction of B cells and their migration to lymphoid tissues. Although we cannot infer the relative contribution of contraction and tissue compartmentalization in the observed loss of memory B cells from blood, nor do we know the vaccination and infection history of our donors, our data indicate that memory B cells are enriched in tissues compared to blood. Accordingly, vaccination in consecutive years induced earlier and larger B cell responses, despite disappearance of vaccine-induced memory from blood. Similarly, robust memory responses were detected after vaccination following B cell depletion by rituximab, implying the presence of memory reservoirs in tissues (*34*). Our data agree with reports on compartmentalization of human virus-specific memory B cells in the spleen (*35*) and distribution of influenza-specific memory B cells across tissues in mice (*36*). Our analysis supports the notion that the assessment of long-term vaccine effectiveness in blood may be suboptimal. Notably, our study suggests that vaccine design needs to consider the localization of memory B cells and the fact that vaccination route affects the B cell response to vaccination (*37*).

Together, we show that activation of cT_{FH} cells, serological memory, and tissue compartmentalization are key factors in human antigen-specific B cell responses. Our study has implications for the design of effective vaccines against influenza viruses and highlights avenues for further research. Specifically, determining ways to activate cT_{FH} cells and $CD8^+$ T cells is of utmost importance. It would be pertinent to understand whether and how the limiting effects of preexisting antibodies on the B cell response can be overcome. Differential compartmentalization of influenza-specific B cell subsets across human tissues and the prominent presence of memory B cells in the lung should be considered with regard to the vaccination route because intranasal vaccination might be more effective in stimulating the influenza-specific memory pool. Further understanding the fate of each B cell population after vaccination will be fundamental to establishing long-lasting serological and cellular immune memory to influenza viruses.

MATERIALS AND METHODS

Study design

This study aimed to dissect the influenza-specific B and T cell responses after vaccination with split inactivated influenza viruses and across human tissues. To that end, 35 healthy adults (>18 years old) were vaccinated over 3 years (2014 to 2016) with the trivalent influenza vaccine (2014, $n = 7$; 2015, $n = 16$) or the 2016 quadrivalent influenza vaccine (2016, $n = 26$), with selected individuals participating in consecutive years (table S1). Peripheral blood samples were collected in heparinized tubes before vaccination (d−1 or d0) and on d7, d14, and d28 after vaccination. For individuals participating in both 2015 and 2016 years, the 2016 baseline sample was used as the 1-year time point (>350 days). Influenza-specific B cells were identified using rHA probes and flow cytometry. ASCs and serum antibody titers were assessed in all three cohorts. cT_{FH} and influenza-specific B cells were assessed in the 2015 and 2016 cohorts. Cellular immunity was assessed in selected donors from the 2014 to 2015 cohort. One donor in the 2016 cohort reported feeling unwell with symptoms of unrelated sickness, and those samples were excluded from analysis. In cases where less than the total number of donors was analyzed, donors were randomly selected for analysis. No other blinding or randomization protocols were applied, and no outliers were excluded. Primary data are reported in table S9.

Human blood and tissue samples

Human experimental work was conducted according to the Declaration of Helsinki Principles and to the Australian National Health and Medical Research Council (NHMRC) Code of Practice. Signed informed consent was obtained from all blood and tissue donors before the study. Tissues from deceased organ donors were obtained after written informed consent from the next of kin. The study was approved by the University of Melbourne Human Ethics Committee (ID 1443389.3 and 1443540), the Mercy Health Human Research Ethics Committee (ID R14/25), and the Australian Red Cross Blood Service (ARCBS) Ethics Committee (ID 2015#8).

Spleen, lung, and lymph node samples were obtained from deceased organ donors. Spleen and lymph node samples were obtained via DonateLife Victoria (table S2). Lung samples were obtained via the Alfred Hospital's Lung Tissue Biobank. Tonsils were obtained from healthy individuals undergoing tonsillectomy (Mater Hospital). PBMCs were isolated from buffy packs obtained from the ARCBS. Umbilical cord blood was obtained via the Mercy Women's Hospital. Bone marrow mononuclear cells, isolated from the posterior ileac crests of healthy volunteers, were commercially purchased (Lonza).

Statistical analysis

Significance was assessed using Wilcoxon matched-pairs signed-rank test (for changes from baseline) or Friedman test (for comparisons between multiple time points). Mann-Whitney test was used to compare unpaired samples, and a paired *t* test was used to compare paired tissue samples. Correlations were assessed using Spearman's correlation coefficient (r_s) for non-Gaussian distributions.

SUPPLEMENTARY MATERIALS

www.sciencetranslationalmedicine.org/cgi/content/full/10/428/eaan8405/DC1

Fig. S1. Gating strategy for circulating ASCs and activated $cT_{FH}1$ cells.
Fig. S2. Specific activation of $cT_{FH}1$ cells after IIV.
Fig. S3. Gating strategy for influenza-specific B cells in PBMC.
Fig. S4. Validation of rHA probe staining.
Fig. S5. BCR analysis of single rHA^+ B cells.
Fig. S6. Frequency of IgA^+ cells in $IgG^-IgD^-IgM^-rHA^+$ B cells in healthy adults.
Fig. S7. Numbers of isotype-specific rHA^+ (H3N2/Swi) B cells.
Fig. S8. rHA^+ B cell kinetics by ELISPOT.
Fig. S9. CD20 expression by $CD21^{lo}CD27^+$ B cells and ASCs.
Fig. S10. Gating strategy for ex vivo live virus ICS.
Fig. S11. Vaccination does not induce $CD8^+$ and innate T cell responses.
Fig. S12. Gating strategy for T cell phenotyping.
Fig. S13. Fold change in influenza-specific B cells during repeated vaccination.
Fig. S14. Validating of rHA probes in human tissues.
Fig. S15. B cell isotype distributions in paired tissue samples.
Table S1. Details of vaccination cohorts.
Table S2. Cohorts of human tissues.

Table S3. FACS panel for ASCs and cT_{FH} cells.
Table S4. FACS panel for influenza-specific T cells after influenza virus infection.
Table S5. FACS panel for phenotyping T cells after vaccination.
Table S6. FACS panel for influenza-specific B cells in 2015 cohort.
Table S7. FACS panel for influenza-specific B cells in 2016 cohort.
Table S8. FACS panel for influenza-specific B cells in human tissues.
Table S9. Primary data.

REFERENCES AND NOTES

1. M. Koutsakos, T. H. O. Nguyen, W. S. Barclay, K. Kedzierska, Knowns and unknowns of influenza B viruses. *Future Microbiol.* **11**, 119–135 (2016).
2. G.-M. Li, C. Chiu, J. Wrammert, M. McCausland, S. F. Andrews, N.-Y. Zheng, J.-H. Lee, M. Huang, X. Qu, S. Edupuganti, M. Mulligan, S. R. Das, J. W. Yewdell, A. K. Mehta, P. C. Wilson, R. Ahmed, Pandemic H1N1 influenza vaccine induces a recall response in humans that favors broadly cross-reactive memory B cells. *Proc. Natl. Acad. Sci. U.S.A.* **109**, 9047–9052 (2012).
3. J. Wrammert, D. Koutsonanos, G.-M. Li, S. Edupuganti, J. Sui, M. Morrissey, M. McCausland, I. Skountzou, M. Hornig, W. I. Lipkin, A. Mehta, B. Razavi, C. Del Rio, N.-Y. Zheng, J.-H. Lee, M. Huang, Z. Ali, K. Kaur, S. Andrews, R. R. Amara, Y. Wang, S. R. Das, C. D. O'Donnell, J. W. Yewdell, K. Subbarao, W. A. Marasco, M. J. Mulligan, R. Compans, R. Ahmed, P. C. Wilson, Broadly cross-reactive antibodies dominate the human B cell response against 2009-pandemic H1N1 influenza virus infection. *J. Exp. Med.* **208**, 181–193 (2011).
4. A. J. McMichael, F. M. Gotch, G. R. Noble, P. A. S. Beare, Cytotoxic T-cell immunity to influenza. *N. Engl. J. Med.* **309**, 13–17 (1983).
5. S. Sridhar, S. Begom, A. Bermingham, K. Hoschler, W. Adamson, W. Carman, T. Bean, W. Barclay, J. J. Deeks, A. Lalvani, Cellular immune correlates of protection against symptomatic pandemic influenza. *Nat. Med.* **19**, 1305–1312 (2013).
6. Z. Wang, Y. Wan, C. Qiu, S. Quiñones-Parra, Z. Zhu, L. Loh, D. Tian, Y. Ren, Y. Hu, X. Zhang, P. G. Thomas, M. Inouye, P. C. Doherty, K. Kedzierska, J. Xu, Recovery from severe H7N9 disease is associated with diverse response mechanisms dominated by $CD8^+$ T cells. *Nat. Commun.* **6**, 6833 (2015).
7. C. Chiu, A. H. Ellebedy, J. Wrammert, R. Ahmed, B cell responses to influenza infection and vaccination. *Curr. Top. Microbiol. Immunol.* **386**, 381–398 (2015).
8. A. H. Ellebedy, R. Ahmed, Re-engaging cross-reactive memory B cells: The influenza puzzle. *Front. Immunol.* **3**, 53 (2012).
9. T. Kurosaki, K. Kometani, W. Ise, Memory B cells. *Nat. Rev. Immunol.* **15**, 149–159 (2015).
10. N. Schmitt, S.-E. Bentebibel, H. Ueno, Phenotype and functions of memory Tfh cells in human blood. *Trends Immunol.* **35**, 436–442 (2014).
11. J. Wrammert, K. Smith, J. Miller, W. A. Langley, K. Kokko, C. Larsen, N.-Y. Zheng, I. Mays, L. Garman, C. Helms, J. James, G. M. Air, J. D. Capra, R. Ahmed, P. C. Wilson, Rapid cloning of high-affinity human monoclonal antibodies against influenza virus. *Nature* **453**, 667–671 (2008).
12. R. Morita, N. Schmitt, S.-E. Bentebibel, R. Ranganathan, L. Bourdery, G. Zurawski, E. Foucat, M. Dullaers, S. Oh, N. Sabzghabaei, E. M. Lavecchio, M. Punaro, V. Pascual, J. Banchereau, H. Ueno, Human blood $CXCR5^+CD4^+$ T cells are counterparts of T follicular cells and contain specific subsets that differentially support antibody secretion. *Immunity* **34**, 108–121 (2011).
13. S.-E. Bentebibel, S. Lopez, G. Obermoser, N. Schmitt, C. Mueller, C. Harrod, E. Flano, A. Mejias, R. A. Albrecht, D. Blankenship, H. Xu, V. Pascual, J. Banchereau, A. Garcia-Sastre, A. K. Palucka, O. Ramilo, H. Ueno, Induction of $ICOS^+CXCR3^+CXCR5^+$ TH cells correlates with antibody responses to influenza vaccination. *Sci. Transl. Med.* **5**, 176ra132 (2013).
14. A. H. Ellebedy, K. J. Jackson, H. T. Kissick, H. I. Nakaya, C. W. Davis, K. M. Roskin, A. K. McElroy, C. M. Oshansky, R. Elbein, S. Thomas, G. M. Lyon, C. F. Spiropoulou, A. K. Mehta, P. G. Thomas, S. D. Boyd, R. Ahmed, Defining antigen-specific plasmablast and memory B cell subsets in human blood after viral infection or vaccination. *Nat. Immunol.* **17**, 1226–1234 (2016).
15. D. Lau, L. Y.-L. Lan, S. F. Andrews, C. Henry, K. T. Rojas, K. E. Neu, M. Huang, Y. Huang, B. DeKosky, A.-K. E. Palm, G. C. Ippolito, G. Georgiou, P. C. Wilson, Low CD21 expression defines a population of recent germinal center graduates primed for plasma cell differentiation. *Sci. Immunol.* **2**, eaai8153 (2017).
16. S. F. Andrews, Y. Huang, K. Kaur, L. I. Popova, I. Y. Ho, N. T. Pauli, C. J. Henry Dunand, W. M. Taylor, S. Lim, M. Huang, X. Qu, J.-H. Lee, M. Salgado-Ferrer, F. Krammer, P. Palese, J. Wrammert, R. Ahmed, P. C. Wilson, Immune history profoundly affects broadly protective B cell responses to influenza. *Sci. Transl. Med.* **7**, 316ra192 (2015).
17. S. F. Andrews, K. Kaur, N. T. Pauli, M. Huang, Y. Huang, P. C. Wilson, High preexisting serological antibody levels correlate with diversification of the influenza vaccine response. *J. Virol.* **89**, 3308–3317 (2015).
18. Y. Li, J. L. Myers, D. L. Bostick, C. B. Sullivan, J. Madara, S. L. Linderman, Q. Liu, D. M. Carter, J. Wrammert, S. Esposito, N. Principi, J. B. Plotkin, T. M. Ross, R. Ahmed, P. C. Wilson, S. E. Hensley, Immune history shapes specificity of pandemic H1N1 influenza antibody responses. *J. Exp. Med.* **210**, 1493–1500 (2013).
19. A. K. Wheatley, A. B. Kristensen, W. N. Lay, S. J. Kent, HIV-dependent depletion of influenza-specific memory B cells impacts B cell responsiveness to seasonal influenza immunisation. *Sci. Rep.* **6**, 26478 (2016).
20. A. K. Wheatley, J. R. R. Whittle, D. Lingwood, M. Kanekiyo, H. M. Yassine, S. S. Ma, S. R. Narpala, M. S. Prabhakaran, R. A. Matus-Nicodemos, R. T. Bailer, G. J. Nabel, B. S. Graham, J. E. Ledgerwood, R. A. Koup, A. B. McDermott, H5N1 vaccine–elicited memory B cells are genetically constrained by the IGHV locus in the recognition of a neutralizing epitope in the hemagglutinin stem. *J. Immunol.* **195**, 602–610 (2015).
21. J. R. R. Whittle, A. K. Wheatley, L. Wu, D. Lingwood, M. Kanekiyo, S. S. Ma, S. R. Narpala, H. M. Yassine, G. M. Frank, J. W. Yewdell, J. E. Ledgerwood, C.-J. Wei, A. B. McDermott, B. S. Graham, R. A. Koup, G. J. Nabel, Flow cytometry reveals that H5N1 vaccination elicits cross-reactive stem-directed antibodies from multiple Ig heavy-chain lineages. *J. Virol.* **88**, 4047–4057 (2014).
22. S. E. Townsend, C. C. Goodnow, R. J. Cornall, Single epitope multiple staining to detect ultralow frequency B cells. *J. Immunol. Methods* **249**, 137–146 (2001).
23. T. Tiller, E. Meffre, S. Yurasov, M. Tsuiji, M. C. Nussenzweig, H. Wardemann, Efficient generation of monoclonal antibodies from single human B cells by single cell RT-PCR and expression vector cloning. *J. Immunol. Methods* **329**, 112–124 (2008).
24. J. L. Halliley, S. Kyu, J. J. Kobie, E. E. Walsh, A. R. Falsey, T. D. Randall, J. Treanor, C. Feng, I. Sanz, F. E.-H. Lee, Peak frequencies of circulating human influenza-specific antibody secreting cells correlate with serum antibody response after immunization. *Vaccine* **28**, 3582–3587 (2010).
25. A. E. Hauser, G. F. Debes, S. Arce, G. Cassese, A. Hamann, A. Radbruch, R. A. Manz, Chemotactic responsiveness toward ligands for CXCR3 and CXCR4 is regulated on plasma blasts during the time course of a memory immune response. *J. Immunol.* **169**, 1277–1282 (2002).
26. N. Wehrli, D. F. Legler, D. Finke, K.-M. Toellner, P. Loetscher, M. Baggiolini, I. C. M. MacLennan, H. Acha-Orbea, Changing responsiveness to chemokines allows medullary plasmablasts to leave lymph nodes. *Eur. J. Immunol.* **31**, 609–616 (2001).
27. M. Odendahl, H. Mei, B. F. Hoyer, A. M. Jacobi, A. Hansen, G. Muehlinghaus, C. Berek, F. Hiepe, R. Manz, A. Radbruch, T. Dörner, Generation of migratory antigen-specific plasma blasts and mobilization of resident plasma cells in a secondary immune response. *Blood* **105**, 1614–1621 (2005).
28. E. J. Kunkel, E. C. Butcher, Plasma-cell homing. *Nat. Rev. Immunol.* **3**, 822–829 (2003).
29. R. S. Herati, A. Muselman, L. Vella, B. Bengsch, K. Parkhouse, D. Del Alcazar, J. Kotzin, S. A. Doyle, P. Tebas, S. E. Hensley, L. F. Su, K. E. Schmader, E. J. Wherry, Successive annual influenza vaccination induces a recurrent oligoclonotypic memory response in circulating T follicular helper cells. *Sci. Immunol.* **2**, eaag2152 (2017).
30. J. S. Tsang, P. L. Schwartzberg, Y. Kotliarov, A. Biancotto, Z. Xie, R. N. Germain, E. Wang, M. J. Olnes, M. Narayanan, H. Golding, S. Moir, H. B. Dickler, S. Perl, F. Cheung; Baylor HIPC Center, CHI Consortium, Global analyses of human immune variation reveal baseline predictors of postvaccination responses. *Cell* **157**, 499–513 (2014).
31. V. I. Zarnitsyna, J. Lavine, A. Ellebedy, R. Ahmed, R. Antia, Multi-epitope models explain how pre-existing antibodies affect the generation of broadly protective responses to influenza. *PLOS Pathog.* **12**, e1005692 (2016).
32. L. Y.-H. Lee, D. L. A. Ha, C. Simmons, M. D. de Jong, N. V. V. Chau, R. Schumacher, Y. C. Peng, A. J. McMichael, J. J. Farrar, G. L. Smith, A. R. M. Townsend, B. A. Askonas, S. Rowland-Jones, T. Dong, Memory T cells established by seasonal human influenza A infection cross-react with avian influenza A (H5N1) in healthy individuals. *J. Clin. Invest.* **118**, 3478–3490 (2008).
33. S. Quinones-Parra, E. Grant, L. Loh, T. H. Nguyen, K. A. Campbell, S. Y. Tong, A. Miller, P. C. Doherty, D. Vijaykrishna, J. Rossjohn, S. Gras, K. Kedzierska, Preexisting $CD8^+$ T-cell immunity to the H7N9 influenza A virus varies across ethnicities. *Proc. Natl. Acad. Sci. U.S.A.* **111**, 1049–1054 (2014).
34. A. Cho, B. Bradley, R. Kauffman, L. Priyamvada, Y. Kovalenkov, R. Feldman, J. Wrammert, Robust memory responses against influenza vaccination in pemphigus patients previously treated with rituximab. *JCI Insight* **2**, 93222 (2017).
35. M. Mamani-Matsuda, A. Cosma, S. Weller, A. Faili, C. Staib, L. Garçon, O. Hermine, O. Beyne-Rauzy, C. Fieschi, J.-O. Pers, N. Arakelyan, B. Varet, A. Sauvanet, A. Berger, F. Paye, J.-M. Andrieu, M. Michel, B. Godeau, P. Buffet, C.-A. Reynaud, J.-C. Weill, The human spleen is a major reservoir for long-lived vaccinia virus–specific memory B cells. *Blood* **111**, 4653–4659 (2008).
36. H. M. Joo, Y. He, M. Y. Sangster, Broad dispersion and lung localization of virus-specific memory B cells induced by influenza pneumonia. *Proc. Natl. Acad. Sci. U.S.A.* **105**, 3485–3490 (2008).
37. H. M. Joo, Y. He, A. Sundararajan, L. Huan, M. Y. Sangster, Quantitative analysis of influenza virus-specific B cell memory generated by different routes of inactivated virus vaccination. *Vaccine* **28**, 2186–2194 (2010).

Acknowledgments: We thank study participants, organ donors, coordinators of DonateLife Victoria for obtaining organ tissues, L. Mariana, and C. Kos for their assistance. We thank DonateLife NSW for paired tissue samples. Lung samples were obtained via the Alfred Hospital's Lung Tissue Biobank, which is supported by the NHMRC Centre of Research Excellence in Lung Fibrosis. We thank N. Bird, K. Watson, M. A. Bernat, L. Carolan, M. Aban, T. Amarasena, and S. Alcantara for their technical assistance. We thank the clinical research midwives G. Christophers, G. Pell, and R. Murdoch for sample collection; and the Obstetrics and Midwifery staff of the Mercy Hospital for Women for their cooperation. We are grateful to A. Ellebedy, R. Ahmed, and C. Vinuesa for providing their expertise. We thank S. Gras and J. Rossjohn (Monash University) for monomers. **Funding:** This work was supported by NHMRC program grants ID1071916 (K.K.) and ID1052979 (S.J.K.) and NHMRC project grants ID1129099 (A.K.W.) and ID1125164 (A.W.C.). M.K. and S.N. are supported by a Melbourne International Research Scholarship and Melbourne International Fee Remission Scholarship (MIFRS). E.B.C. is an NHMRC Peter Doherty Fellow. S.S. is supported by the Victoria-India Doctoral Scholarship and MIFRS. World Health Organization (WHO) Collaborating Centre for Reference Research on Influenza is supported by the Australian Government Department of Health. S.I.M. is supported by Juvenile Diabetes Research Foundation (JDRF) Career Development Award (5-CDA-2014-210-A-N) and NHMRC (ID1123586). M.L. is supported by a Career Development Fellowship from NHMRC (ID1047025). S.R. is an employee of Seqirus Ltd. S.G.T. is supported by NHMRC program and project grants. S.G.T., S.J.K., and K.K. are NHMRC Research Fellows. **Author contributions:** M.K., T.H.O.N., and K.K. designed experiments. M.K., A.K.W., A.F., and T.H.O.N. performed experiments. M.K., L.L., E.B.C., S.S., S.N., and T.H.O.N. processed blood and tissues. K.L.L. and A.C.H. performed serological analysis. M.L., T.L., S.I.M., G.P.W., L.M.W., M.E., and S.G.T. obtained and provided tissues. A.K.W. and S.J.K. generated rHA probes. M.K., A.W.C., T.H.O.N., and K.K. analyzed data. M.K., T.H.O.N., and K.K. wrote the manuscript. All authors revised the manuscript. **Competing interests:** S.R. holds shares in CSL Ltd., the parent company to Seqirus, which is the manufacturer of influenza vaccines (Afluria, Agripal, Flucelvax, FluAd) received by some, but not all, of the participants of this study. The other authors declare that they have no competing interests.

Submitted 26 May 2017
Resubmitted 5 September 2017
Accepted 22 December 2017
Published 14 February 2018
10.1126/scitranslmed.aan8405

Citation: M. Koutsakos, A. K. Wheatley, L. Loh, E. B. Clemens, S. Sant, S. Nüssing, A. Fox, A. W. Chung, K. L. Laurie, A. C. Hurt, S. Rockman, M. Lappas, T. Loudovaris, S. I. Mannering, G. P. Westall, M. Elliot, S. G. Tangye, L. M. Wakim, S. J. Kent, T. H. O. Nguyen, K. Kedzierska, Circulating T_{FH} cells, serological memory, and tissue compartmentalization shape human influenza-specific B cell immunity. *Sci. Transl. Med.* **10**, eaan8405 (2018).

Science Translational Medicine

Circulating T_{FH} cells, serological memory, and tissue compartmentalization shape human influenza-specific B cell immunity

Marios Koutsakos, Adam K. Wheatley, Liyen Loh, E. Bridie Clemens, Sneha Sant, Simone Nüssing, Annette Fox, Amy W. Chung, Karen L. Laurie, Aeron C. Hurt, Steve Rockman, Martha Lappas, Thomas Loudovaris, Stuart I. Mannering, Glen P. Westall, Michael Elliot, Stuart G. Tangye, Linda M. Wakim, Stephen J. Kent, Thi H. O. Nguyen and Katherine Kedzierska

Sci Transl Med **10**, eaan8405.
DOI: 10.1126/scitranslmed.aan8405

Investigating influenza immunity

Seasonal influenza vaccines have been recommended for decades, but studies focused on antigen-specific lymphocytes in humans are sparse. Koutsakos *et al.* examined longitudinal samples of influenza-vaccinated individuals to determine what responses generate protective immunity. Vaccination could induce circulating T follicular helper memory cells, antibody-secreting cells, and memory B cells, but did not seem to affect other types of lymphocytes. Existing anti-influenza antibodies at the time of vaccination dampened these responses. They probed different types of human tissues to hunt for influenza memory B cells, thereby showing that the memory response exists outside the circulation. Better targeting these cells could improve influenza vaccine efficacy.